Cell Metabolism
Article

Hypothalamic CaMKK2 Contributes to the Regulation of Energy Balance

Kristin A. Anderson,[1] Thomas J. Ribar,[1] Fumin Lin,[1] Pamela K. Noeldner,[1] Michelle F. Green,[1] Michael J. Muehlbauer,[2] Lee A. Witters,[3] Bruce E. Kemp,[4] and Anthony R. Means[1,*]
[1]Department of Pharmacology and Cancer Biology
[2]Sarah W. Stedman Nutrition and Metabolism Center
Duke University School of Medicine, Durham, NC 27710, USA
[3]Departments of Medicine and Biochemistry, Dartmouth Medical School and Department of Biological Sciences, Dartmouth College, Hanover, NH 03755, USA
[4]St. Vincent's Institute of Medical Research, CSIRO Molecular and Health Technologies, and University of Melbourne, Fitzroy, Victoria 3065, Australia
*Correspondence: means001@mc.duke.edu
DOI 10.1016/j.cmet.2008.02.011

SUMMARY

Detailed knowledge of the pathways by which ghrelin and leptin signal to AMPK in hypothalamic neurons and lead to regulation of appetite and glucose homeostasis is central to the development of effective means to combat obesity. Here we identify CaMKK2 as a component of one of these pathways, show that it regulates hypothalamic production of the orexigenic hormone NPY, provide evidence that it functions as an AMPKα kinase in the hypothalamus, and demonstrate that it forms a unique signaling complex with AMPKα and β. Acute pharmacologic inhibition of CaMKK2 in wild-type mice, but not *CaMKK2* null mice, inhibits appetite and promotes weight loss consistent with decreased *NPY* and *AgRP* mRNAs. Moreover, the loss of CaMKK2 protects mice from high-fat diet-induced obesity, insulin resistance, and glucose intolerance. These data underscore the potential of targeting CaMKK2 as a therapeutic intervention.

INTRODUCTION

Obesity and associated diseases such as type 2 diabetes, hypertension, cardiovascular disorders, and some cancers are a threat to general human health and have stimulated increased interest in understanding the molecular mechanisms responsible for coordinated food intake, body weight, and glucose homeostasis (Zamboni et al., 2005). Recent findings have emphasized the role of the central nervous system (CNS), especially the hypothalamus, in integrating hormonal and nutrient signals from the periphery to modulate food intake, energy expenditure, and peripheral glucose metabolism (Morton et al., 2006). For example, abundant evidence indicates that the CNS is the site for the appetite-controlling actions of leptin. Much progress has been made in identifying neuronal populations in the arcuate nucleus (ARC) and ventromedial hypothalamus (VMH) of the hypothalamus that are directly responsive to leptin; the signaling steps leading to transcriptional activation upon engagement of the leptin receptor; and the neuronal circuitry linking leptin-responsive neurons with populations of neurons that underlie leptin's endocrine, autonomic, and behavioral effects (Elmquist et al., 2005; Flier, 2004; Friedman and Halaas, 1998). Unfortunately, while administration of leptin causes weight loss in lean mammals, there is typically leptin resistance in obese individuals that compromises the use of leptin to treat obesity (Heymsfield et al., 1999).

An emerging view holds that common neuronal circuitry is used by a variety of hormones and metabolites that affect energy homeostasis. One especially important example is ghrelin, which is produced by the stomach and opposes the hypothalamic actions of leptin by stimulating food intake. Plasma ghrelin levels display an episodic secretory pattern, rising shortly before meals and falling sharply on feeding (Bagnasco et al., 2002). Ghrelin also rises with acute fasting or chronic food deprivation and in response to weight loss due to chronic exercise, eating disorders, and cancer anorexia. Notably, the same effect occurs following diet-induced weight loss, suggesting a mechanism for the rebound weight gain following dieting (Cummings et al., 2002). It is through the upregulation of NPY and AgRP, the most potent physiological appetite transducers known in mammals, that ghrelin mediates its effect on food intake (Kalra and Kalra, 2004). Ghrelin binds the Gq-coupled growth hormone secretagogue receptor expressed on NPY neurons in the ARC, which leads to the increase in intracellular Ca^{2+} required for transcriptional activation of the *NPY* and *AgRP* genes (Holst et al., 2005; Kohno et al., 2003; Kojima et al., 1999; Sun et al., 2004). Administration of NPY to rodents rapidly causes voracious feeding and leads to increased adiposity over prolonged periods (Clark et al., 1984). Blocking NPY action or selectively ablating NPY neurons in rodents suppresses feeding and reduces obesity and fasting-induced responses (Broberger and Hokfelt, 2001; Gropp et al., 2005; Luquet et al., 2005). In some situations, inhibition of NPY signaling reduces food intake and body weight without cachexia or rebound weight gain (Lambert et al., 2001). These observations have prompted efforts to design antagonists to NPY and to NPY receptors as therapeutics. However, poor bioavailability and brain penetration and nonselective nature of action have thus far confounded development of an effective

therapeutic and have underscored the need to identify additional signaling components in the pathway (Kalra and Kalra, 2004).

Recently, the AMP-dependent protein kinase (AMPK) was identified as one such signaling component. The intraperitoneal (i.p.) or intracerebroventricular (i.c.v.) injection of ghrelin in rodents increases the phosphorylation and activation of AMPK in the hypothalamus, while i.c.v. administration of a pharmacological AMPK activator (AICAR) stimulates food intake and body weight gain in these animals (Andersson et al., 2004; Kola et al., 2005). In addition, analysis of dissected hypothalami has demonstrated a correlation between altered levels of AMPK activity and expression of NPY (Minokoshi et al., 2004). Collectively, the data indicate a role for AMPK in NPY neurons, downstream of ghrelin and upstream of *NPY* gene expression and the stimulation of appetite.

The AMPK holoenzyme is a heterotrimer comprised of α catalytic and β and γ regulatory subunits and requires phosphorylation of the α subunit on Thr172 by an upstream activating kinase for activity (Hardie et al., 2003). Numerous studies indicate that the tumor suppressor protein LKB1, mutations of which lead to Peutz-Jeghers syndrome, is the relevant AMPK kinase (AMPKK) when AMPK is responding to acute changes in energy balance that occur at the cellular level (Sakamoto et al., 2005; Shaw et al., 2004, 2005). In this context, AMPK activation also requires 5′-AMP, which binds the γ regulatory subunit and allosterically activates the kinase, while at the same time inhibiting dephosphorylation of Thr172 by PP2C. Thus, an increase in the AMP/ATP ratio that occurs when ATP levels are depleted is sensed by AMPK. Once activated, AMPK switches off anabolic pathways and other processes that consume ATP, such as lipid and carbohydrate synthesis, while switching on catabolic pathways that generate ATP, such as fatty acid oxidation and glucose uptake, in order to restore energy balance. The AMP/LKB1-dependent activation of AMPK results from pathological stresses such as heat shock, hypoxia, and glucose deprivation and is responsible for mediating activation of AMPK by the antidiabetic drug metformin. Physiological stimuli such as contraction-stimulated glucose uptake by muscle cells and glucose homeostasis in liver also depend on this pathway. Thus, in peripheral tissues, it is desirable to activate AMPK.

Recently, the Ca^{2+}/calmodulin (CaM)-dependent protein kinase kinases (CaMKK) were shown to function as physiologically relevant AMPK kinases in cells, observations that have broadened the scope of AMPK regulation (Hawley et al., 2005; Hurley et al., 2005; Woods et al., 2005). In contrast to that directed by AMP/LKB1, the CaMKK-dependent activation of AMPK operates independently of AMP, instead requiring a change in intracellular Ca^{2+}. The abundant expression of CaMKK in brain led us to predict that Ca^{2+}/CaM/CaMKK may regulate the phosphorylation of AMPK in NPY neurons of the hypothalamus and that, if so, it would be desirable to inactivate AMPK in this tissue (Witters et al., 2006).

Here we show that primary defects in mice null for *CaMKK2* are reduced hypothalamic AMPK activity and downregulation of *NPY* and *AgRP* gene expression in NPY neurons. Acute i.c.v. administration of a CaMKK antagonist to wild-type mice, but not *CaMKK2* null mice, results in decreased food intake that correlates with decreased hypothalamic *NPY* and *AgRP* mRNAs. Intriguingly, the absence of CaMKK2 also protects mice from diet-induced weight gain, hyperglycemia, and insulin resistance, and we infer that the mechanism involved may also involve hypothalamic AMPK. Finally, we identify and characterize a unique complex comprised of CaMKK2, AMPKα/β, and Ca^{2+}/CaM that may be the physiologically relevant signaling complex for mediating these central effects on energy homeostasis.

RESULTS

CaMKK2 Regulates NPY in the Hypothalamus

CaMKK2 is expressed throughout the brain, although its presence in hypothalamus has not been specifically examined (Anderson et al., 1998). Immunoblotting of hypothalamic extracts from wild-type (WT) mice revealed that CaMKK2 protein is present in this part of the brain (Figure 1A) and appears as a doublet, consistent with findings in HeLa cells (Hurley et al., 2005). The hypothalamus is divided into regions including the ARC, VMH, and lateral hypothalamus (LH), each with unique functions and all previously shown to express AMPK. To identify regions where CaMKK2 might colocalize with AMPK and function as an AMPKK, its expression pattern in the hypothalamus was examined by in situ hybridization. Coronal sections of adult mouse brain were collected from the midregion of the hypothalamus and incubated with antisense riboprobes designed to hybridize with *MCH*, *NPY*, or *CaMKK2* mRNAs. NPY and MCH are neuropeptides expressed within neurons present only in the ARC or VMH, respectively, and served as positive controls. Consistent with previous studies in rat brain, *CaMKK2* signal was strong in the hippocampus and cortex and was shown here to be present in the hypothalamus, where it appeared largely restricted to the ARC (Figure 1B). Compared to *NPY*, *CaMKK2* expression is observed throughout a larger region, suggesting its presence in multiple cell types. When mRNA levels were quantified from ARC punches, *CaMKK2*, *NPY*, *AgRP*, and *POMC* were found to be enriched 20- to 40-fold relative to whole hypothalamus (Figure 1C). In contrast, MCH was barely detectable. Hypothalamic punches that failed to display enrichment for *NPY* showed correspondingly reduced levels of *CaMKK2* (data not shown). This finding, together with the in situ hybridization result, is consistent with localization of CaMKK2 to NPY and POMC neurons present in the ARC; however, it cannot provide unequivocal assignment of CaMKK2 to specific neuron types. To evaluate the possibility of a functional correlation between CaMKK2 and NPY, we compared hypothalamic *NPY*, *AgRP*, and *POMC* mRNA levels in WT and *CaMKK2* null mice. Figure 1D shows decreased *NPY* and *AgRP* levels in the mutant, but no significant difference in *POMC*. These results implicate CaMKK2 in a pathway that regulates NPY and AgRP in NPY neurons.

Since CaMKK2 can function as an AMPK in cells, we questioned whether the absence of CaMKK2 alters hypothalamic AMPK activity. AMPK was immunoprecipitated from protein extracts prepared from WT and *CaMKK2* null mice and assayed in vitro. A statistically significant decrease in AMPK activity was observed in the *CaMKK2* null samples (Figure 1E), consistent with diminished AMPK-NPY signaling. We suspect that the modest decrease in total hypothalamic AMPK activity reflects the observation that *CaMKK2* expression is restricted to a small region of the hypothalamus and is considerably enriched in

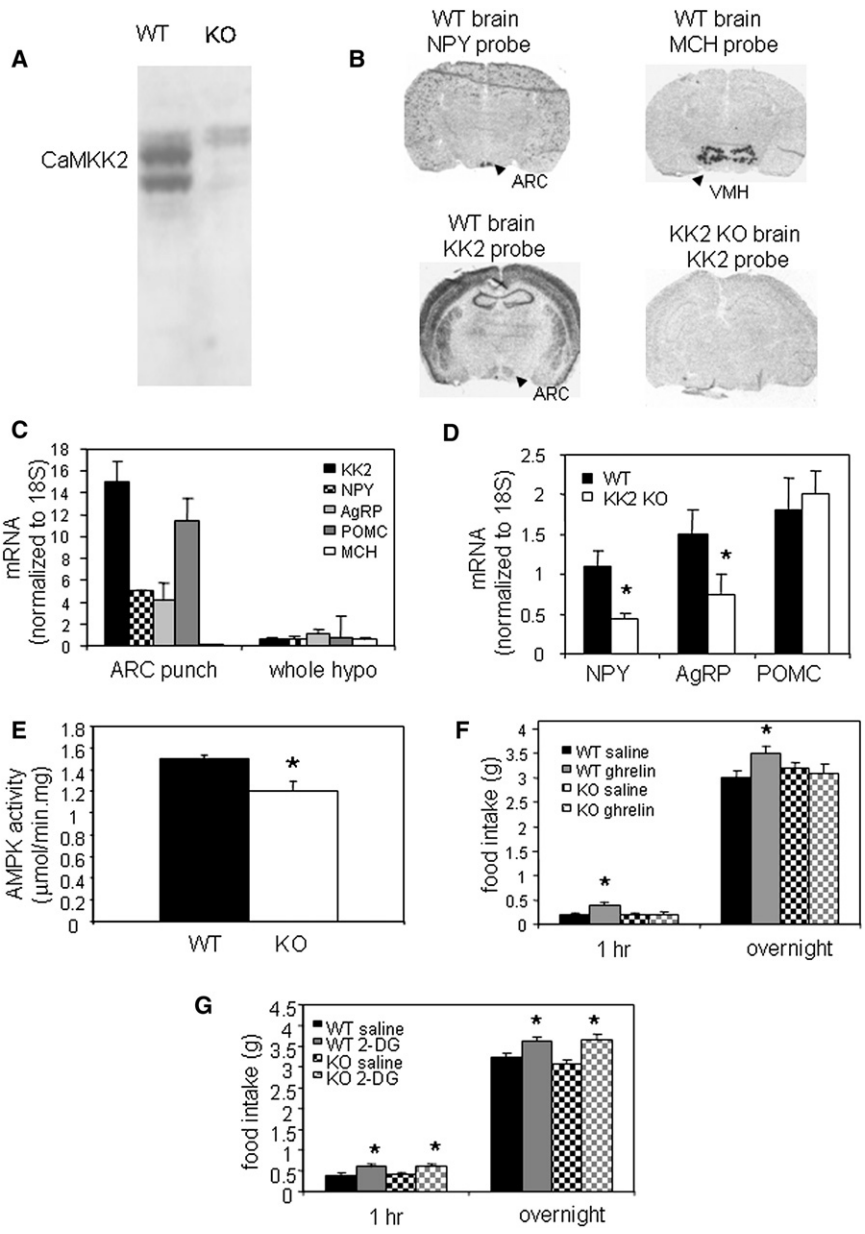

Figure 1. CaMKK2 Is Expressed in the Hypothalamus and Regulates NPY

(A) CaMKK2 protein is expressed in the hypothalamus. Protein extracts of hypothalamus from wild-type (WT) and *CaMKK2* null (KO) mice were immunoblotted for CaMKK2. CaMKK2 protein appears as a doublet in the WT sample and is absent from the KO sample.

(B) *CaMKK2* mRNA is expressed in the hypothalamus. Coronal mouse brain sections collected at the midregion of the hypothalamus were incubated as indicated with antisense riboprobes against *NPY* and *MCH*, which serve as positive controls for the arcuate nucleus (ARC) and ventromedial hypothalamus (VMH), respectively, and against *CaMKK2*.

(C) *CaMKK2*, *NPY*, *AgRP*, and *POMC* mRNAs are enriched in ARC punch biopsies from hypothalamus of WT mice. n = 3.

(D) *NPY* and *AgRP* mRNA levels are decreased in hypothalamus of *CaMKK2* null mice. Total RNA was isolated from hypothalamus of WT and *CaMKK2* null mice that had been fasted overnight, and *NPY*, *AgRP*, and *POMC* mRNA levels were quantified by RT-PCR. n = 8; *$p < 0.05$.

(E) AMPK activity is decreased in hypothalamus of *CaMKK2* null mice. Following immunoprecipitation of AMPK from hypothalamic extracts of fasted WT and *CaMKK2* null mice, AMPK activity was determined in vitro with SAMS peptide as substrate. A representative experiment is shown. n = 4; *$p < 0.05$.

(F) Food intake of *CaMKK2* null mice is unaffected by exogenously administered ghrelin. WT and *CaMKK2* null mice were given intraperitoneal (i.p.) injections of saline or ghrelin (3 nmol/100 μl per mouse) 1 hr before onset of dark cycle, and food intake was quantified at 1 hr and overnight. n = 11 (WT), n = 12 (*CaMKK2* null); *$p < 0.05$.

(G) Food intake of *CaMKK2* null and WT mice is affected similarly by 2-DG. In the control experiment, mice were given i.p. injections of 2-deoxyglucose (2-DG) at a dose of 15 mg/100 μl per mouse, and food intake was monitored as in (F). n = 11 (WT), n = 12 (*CaMKK2* null); *$p < 0.05$.

Data are presented as means ± SEM.

punch biopsies containing ARC (Figures 1B and 1C), whereas AMPK activity is detected throughout the hypothalamus (Minokoshi et al., 2004).

Ghrelin stimulates food intake via binding to growth hormone secretagogue receptors (GHS-Rs) present on NPY neurons, which leads to an increase in intracellular Ca^{2+} and activation of the AMPK-NPY pathway (Cummings et al., 2005). This signaling pathway was further evaluated by systemic administration of ghrelin to WT and *CaMKK2* null mice. Ghrelin increased food intake of WT animals at 1 hr and overnight but had no effect on food intake of *CaMKK2* null mice (Figure 1F). The ghrelin signal can be bypassed by 2-deoxyglucose (2-DG), which causes AMP/LKB1-dependent activation of AMPK due to depletion of cellular energy stores, which raises the AMP/ATP ratio. As shown in Figure 1G, systemic administration of 2-DG stimulated the food intake of both WT and *CaMKK2* null mice to the same extent. Collectively, our data are consistent with a signaling defect in the NPY neurons of *CaMKK2* null mice lying downstream of ghrelin and upstream of AMPK that affects the expression of *NPY* and *AgRP* mRNAs.

STO-609 Blocks Ca^{2+}-Dependent Induction of NPY

As we wanted to provide more direct evidence linking CaMKK2, AMPK, and NPY production, we turned to N38 cells, an immortalized cell line derived from mouse hypothalamus that have been shown to express NPY. These cells express CaMKK2 (Figure 2A) and other components of the AMPK signaling pathway that can be activated by treating the cells with exogenous stimuli. Ionomycin, which increases intracellular Ca^{2+} leading to activation of CaMKK2, and 2-DG, which raises the AMP/ATP ratio by inhibiting cellular production of ATP, both result in increased levels of phosphorylated AMPK (p-AMPK) and

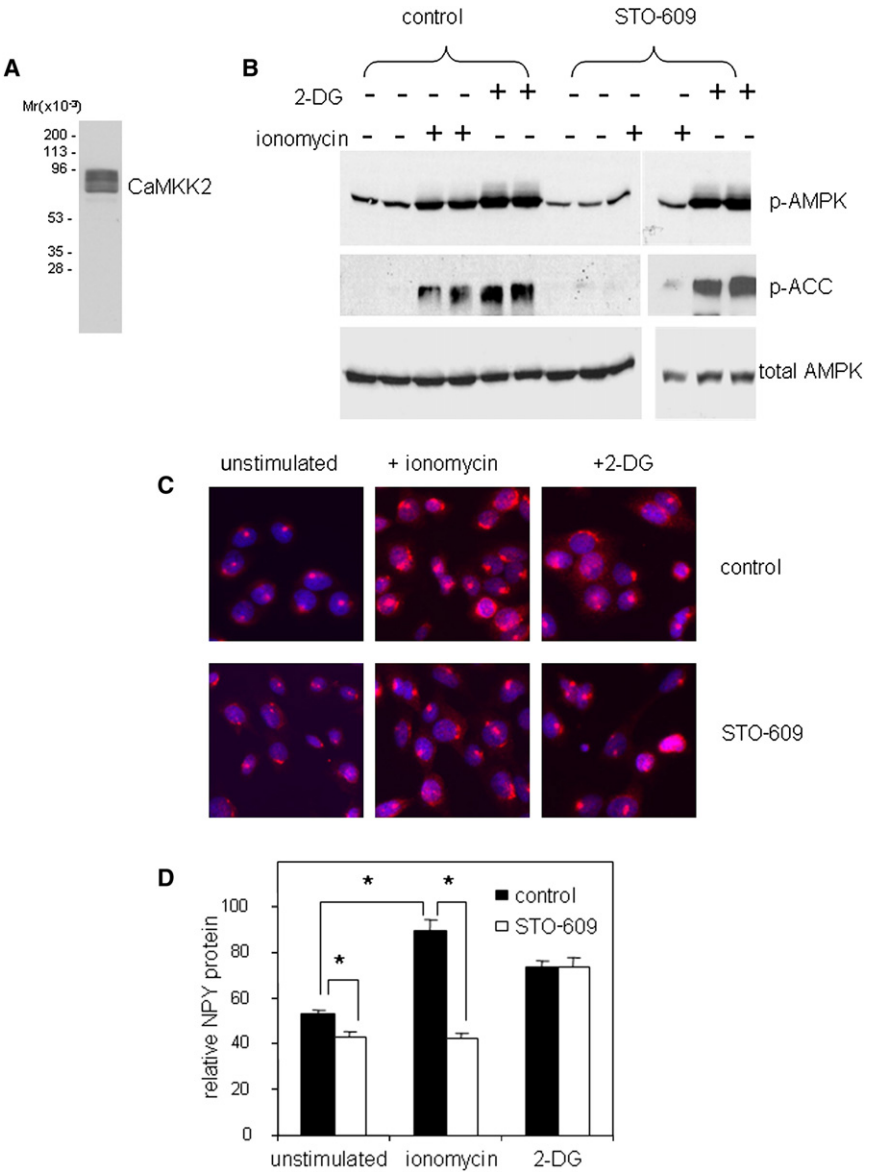

Figure 2. Ca^{2+}-Dependent Induction of *NPY* Expression in N38 Cells Is Blocked by STO-609

(A) CaMKK2 protein is detected in N38 cell protein extracts by immunoblotting.

(B) N38 cells were incubated for 1 hr with vehicle or with 10 μM STO-609, followed by stimulation with 1 μM ionomycin for 5 min or 50 mM 2-DG for 15 min. Cell extracts were prepared and immunoblotted for phosphorylated AMPK (p-AMPK), total AMPK, and p-ACC. STO-609 selectively blocks the ionomycin-induced increase in p-AMPK and p-ACC. One representative experiment is shown.

(C) N38 cells were incubated for 1 hr with vehicle or with 10 μM STO-609, followed by stimulation with 1 μM ionomycin or with 50 mM 2-deoxy glucose (2-DG) for 6 hr. The cells were then fixed, and the NPY protein signal (red) was visualized by immunocytochemistry. The cells were costained with the DAPI nuclear marker (blue). One representative experiment is shown. n = 3.

(D) NPY signal intensity in (C) was quantified using MetaMorph version 7.1 software. Forty cells were analyzed for each condition. Shown are means ± SEM. n = 40; *p < 0.0002.

p-ACC (Figure 2B). The selective CaMKK2 inhibitor STO-609 blocks the ionomycin-induced increases in p-AMPK and p-ACC, but not the phosphorylation of these proteins in response to 2-DG (Figure 2B). We used immunocytochemistry to show that ionomycin increases the amount of NPY in N38 cells and that this increase is prevented by the selective CaMKK inhibitor STO-609 (Tokumitsu et al., 2002) (Figures 2C and 2D). These data support our contention that a rise in Ca^{2+} results in activation of CaMKK2, which in turn phosphorylates AMPK, leading to an increase in NPY.

Depletion or Inhibition of CaMKK2 Inhibits Food Intake

NPY is a well-established potent orexigenic factor, and depleting NPY signaling in mice reduces refeeding after a fast. This phenotype is most severe during the first hour of the refeeding period and gradually returns to normal by 24 hr (Segal-Lieberman et al., 2003). When refeeding behavior was examined in *CaMKK2* null animals, they were found to exhibit a defect similar to that previously reported for *NPY*-depleted mice (Figure 3A). After a 48 hr fast, *CaMKK2* null mice ate less than WT mice during a 6 hr refeeding period, with the greatest decrease in food intake occurring at the early time points, but by 48 hr the difference was abrogated (Figure 3A). Figure 3B shows the food intake of nonfasted wild-type and *CaMKK2* null control animals over a 48 hr period.

Intracerebroventricular administration of NPY to rats leads to robust induction of food intake, while chronic infusion results in increased adiposity and insulin resistance (Clark et al., 1984), and ablation of NPY neurons in adult mice induces life-threatening anorexia (Gropp et al., 2005; Luquet et al., 2005). The hypothesis that CaMKK2 controls appetite by regulating *NPY* gene expression in the hypothalamus predicts that acute inhibition of CaMKK2 in adult WT animals should decrease appetite. To test this idea, the selective CaMKK inhibitor STO-609 (Tokumitsu et al., 2002) was administered i.c.v. to adult male WT mice, and the effect on appetite was assessed by quantifying food intake. Compared to animals receiving saline, the WT STO-609 group ate significantly less food during the 6 days over which food intake was monitored (Figure 3C) and also lost body weight (Figure 3E). We repeated the food intake experiment using adult male *CaMKK2* null mice. Whereas the *CaMKK2* mice receiving vehicle consumed food to the same extent as similarly treated WT mice, STO-609 did not alter the feeding behavior or decrease the body weight of *CaMKK2* null mice (Figures 3D and 3F). As predicted, the WT animals receiving STO-609 also exhibited decreased hypothalamic *NPY* and *AgRP* mRNAs compared to

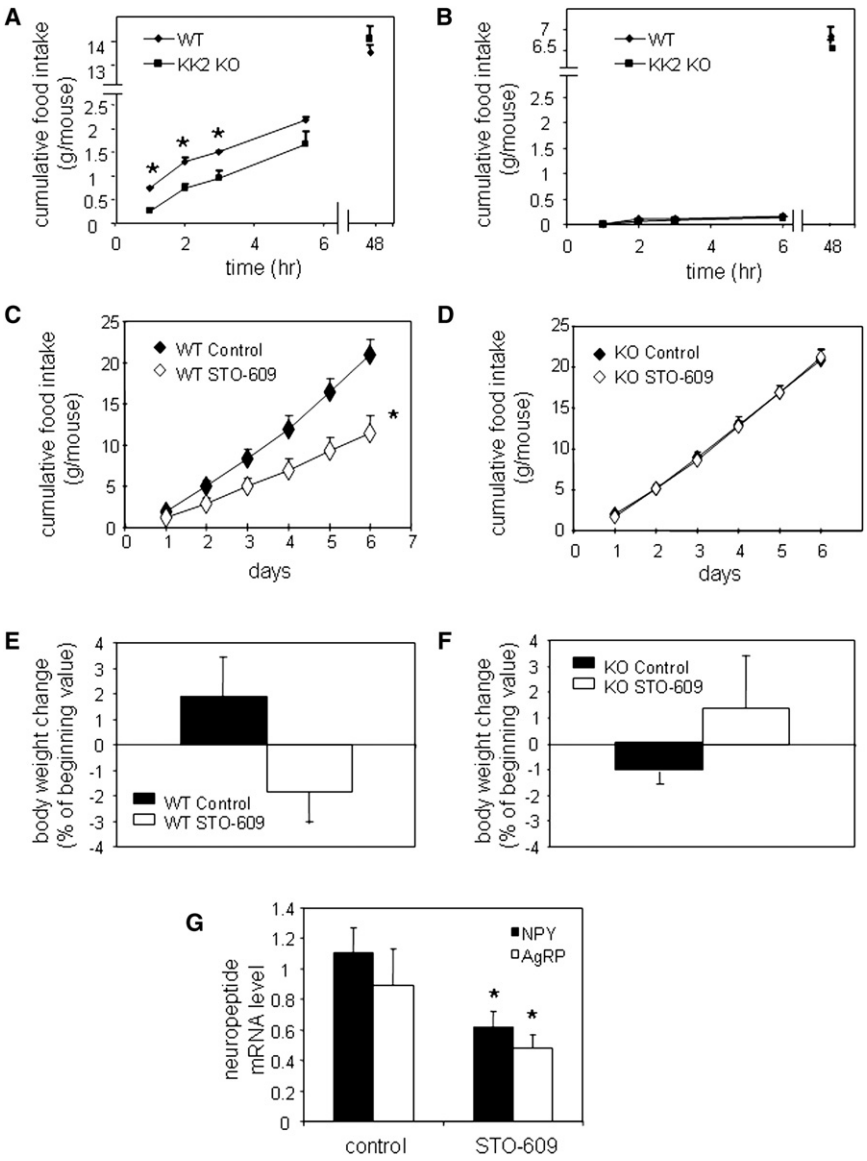

Figure 3. Depletion or Inhibition of CaMKK2 Inhibits Food Intake

(A) *CaMKK2* null mice display reduced refeeding after a fast. Food intake was quantified hourly during a 6 hr refeeding period and at 48 hr, following a 48 hr fast. n = 7; *p < 0.02.

(B) In the control experiment, the food intake of nonfasted animals was measured.

(C and D) Intracerebroventricular (i.c.v.) administration of STO-609 to WT mice, but not to *CaMKK2* null mice, decreases food intake. STO-609 was administered i.c.v. to WT and *CaMKK2* null mice continuously for 6 days at a concentration of 20 μM and a rate of 0.5 μl/hr, during which time food intake was measured daily. Cumulative food intake is shown. n = 9; *p < 0.05 (C); n = 10 (D).

(E and F) Change in body weight by the end of the 6 day experiment is plotted as a percentage of the starting value obtained before the cannulation surgery. n = 7.

(G) At the end of the experiment, WT animals were sacrificed, and hypothalamic *NPY* and *AgRP* mRNAs were quantified by real-time PCR. n = 7; *p < 0.05.

Data are presented as means ± SEM.

controls (Figure 3G). The effects of STO-609 on food intake and *NPY* and *AgRP* mRNA expression in WT mice, but not *CaMKK2* null mice, provide compelling independent evidence that CaMKK2 signaling is required for appetite control.

CaMKK2$^{-/-}$ Mice Are Resistant to a High-Fat Diet

Diminished NPY signaling in *CaMKK2*$^{-/-}$ mice suggests that these animals will eat less due to decreased appetite and accumulate less body weight over time. To test this idea, we utilized the Surwit diet, a calorie-paired low-fat/high-fat diet that is commonly referred to as the diet-induced obese model and that was developed for C57BL/6J mice, the predominant genetic background of our mice (Petro et al., 2004; Surwit et al., 1988). For this experiment, WT and *CaMKK2*$^{-/-}$ mice were fed either a low-fat control diet (D12328 CCO) or the high-fat equivalent of this diet (D12330 HCO) from weaning (3 weeks of age) to 34 weeks of age. As shown in Figure 4, the body weight gain of *CaMKK2*$^{-/-}$ mice as monitored during the 31 weeks was significantly decreased compared to WT controls for animals fed low-fat chow (Figure 4A), and this difference was enhanced for animals maintained on high-fat chow (Figure 4B). Consistent with the observed reduction in body weight, *CaMKK2* null mice displayed a reduced average daily food intake over the course of the experiment and a reduction in adiposity measured after 31 weeks on either diet (Figures 4C and 4D).

After 31 weeks on the two diets, the ability of the animals to handle glucose was evaluated. Glucose tolerance testing revealed that WT mice on the high-fat diet had become less tolerant compared with WT animals maintained on low-fat chow (Figures 4E and 4F). The observed increase in glucose excursion exhibited by WT mice fed high-fat chow is typical of that previously attributed to a diet-induced change (Petro et al., 2004; Surwit et al., 1988). *CaMKK2*$^{-/-}$ mice on low-fat chow responded to glucose similarly to WT mice on low-fat chow. However, unlike WT animals, the *CaMKK2*$^{-/-}$ mice retained the low-fat-diet-like response to glucose even when fed high-fat chow for 31 weeks (Figures 4E and 4F). After 1 week of recovery, the same group of animals was tested for insulin sensitivity. Consistent with the results from the glucose tolerance testing, WT mice had developed the predicted increase in insulin resistance, whereas *CaMKK2* null animals were protected from diet-induced changes in insulin action (Figures 4G and 4H).

After an additional several weeks of recovery, the animals were sacrificed and serum levels of ghrelin and leptin were quantified. As shown in Figure 4I, *CaMKK2*$^{-/-}$ animals did not exhibit a decrease in ghrelin levels, indicating their ability to synthesize and secrete ghrelin. In fact, ghrelin levels were increased in *CaMKK2*

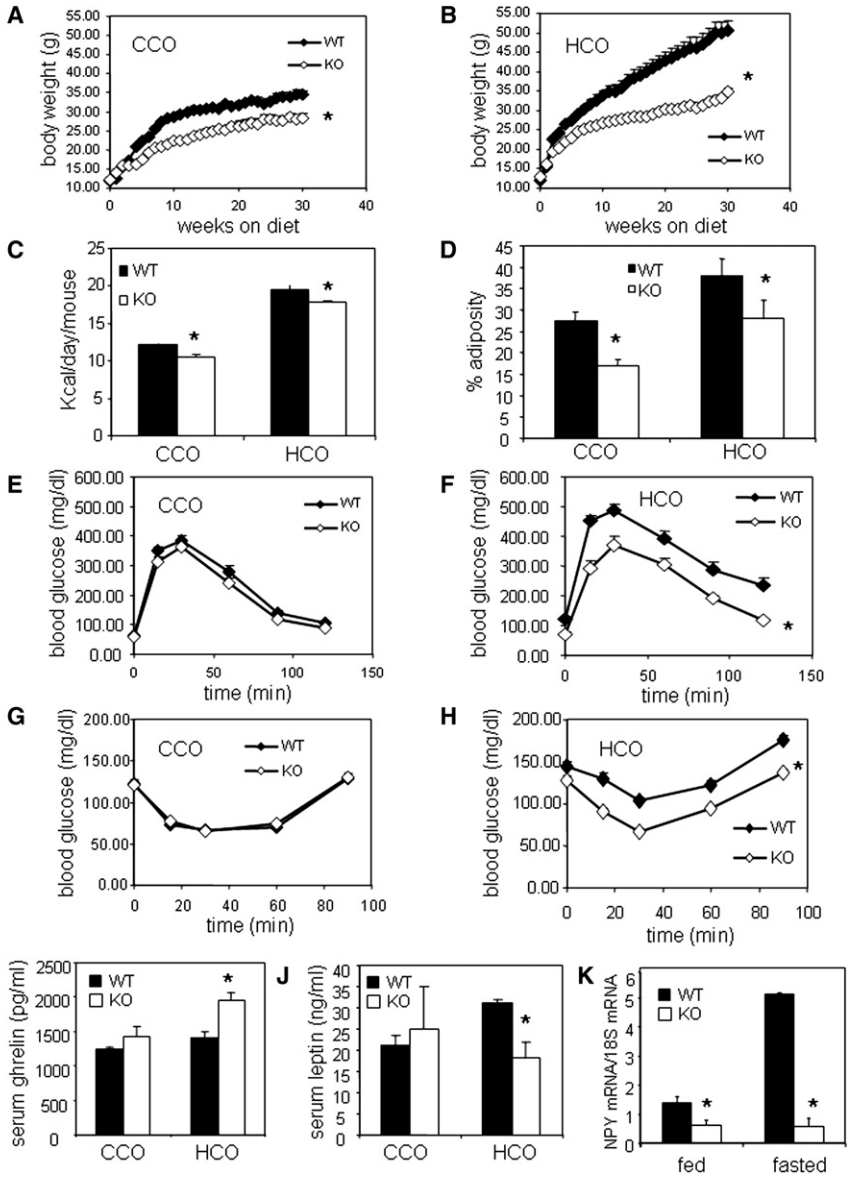

Figure 4. *CaMKK2* Null Mice Consume Less Food and Are Resistant to High-Fat Diet-Induced Adiposity, Glucose Intolerance, and Insulin Resistance

Twenty male WT and *CaMKK2* null mice were housed five per cage at the age of weaning and fed control (D12328) or high-fat (D12330) diets from Research Diets for 31 weeks. Measurements of food intake and weight gain were performed weekly.

(A and B) Growth curves of the two groups on both diets show that the *CaMKK2* null mice gain significantly less weight than the WT mice. *$p < 0.01$ by one-way ANOVA.

(C) Average daily food intake of *CaMKK2* null mice is reduced compared to control animals. *$p < 0.02$.

(D) Dual energy X-ray absorptiometry (DEXA) scans of *CaMKK2* null mice indicate a significant decrease in adiposity compared to WT animals after 31 weeks on either control or high-fat diet. *$p < 0.02$.

(E–H) On the high-fat diet, *CaMKK2* null mice also remain glucose tolerant (E and F) and insulin sensitive (G and H) relative to WT mice. *$p < 0.01$.

(I and J) After 31 weeks on low-fat ($n = 5$) or high-fat ($n = 10$) diet, WT and *CaMKK2* null mice were sacrificed, and total serum ghrelin (I) and leptin (J) levels were quantified. *$p < 0.05$.

(K) After 31 weeks on high-fat chow, WT and *CaMKK2* null mice were either fasted overnight or fed ad libitum. The animals were then sacrificed, and hypothalamic *NPY* mRNA levels were quantified by real-time PCR. $n = 4$; *$p < 0.02$.

Data are presented as means ± SEM.

null mice, suggesting the possibility that these mice attempt to compensate for a defect in the ghrelin signaling pathway by increasing its production. Consistent with this idea, serum leptin was decreased in *CaMKK2* null mice (Figure 4J). This also follows from the defect in the ghrelin pathway, as the NPY neurons would respond to a decrease in ghrelin activity as if there had been an increase in leptin. Indeed, hypothalamic *NPY* mRNA was decreased in the *CaMKK2* null mice fed the high-fat diet relative to WT mice, and the decrease was accentuated upon fasting (Figure 4K). Together, these data are consistent with our observations in Figure 1 that *CaMKK2* null mice cannot respond to ghrelin with the appropriate increase in feeding and body weight gain and that this may be due in part to decreased production of NPY.

CaMKK2 and AMPK Form a Signaling Complex

A central tenet of signal transduction is that the appropriate propagation of signals along a pathway often depends on formation of a complex of its components. To determine whether CaMKK2 associates with AMPK, the AMPKα subunit was immunoprecipitated from mouse brain extract and probed for CaMKK2. CaMKK2 does coprecipitate with AMPKα from mouse brain (Figure 5A). The interaction was further characterized using a FLAG-tagged version of CaMKK2 overexpressed in HEK293A cells, which represents a convenient cell-based system. The transfected FLAG-CaMKK2 appears to be functionally linked to AMPK, as both basal and ionomycin-induced phosphorylation of AMPK were increased by the presence of the kinase (Figure 5B). Moreover, endogenous AMPK and FLAG-CaMKK2 associate in HEK293A cells, as p-AMPK coimmunoprecipitated with FLAG-CaMKK2 (Figure 5C). Also detected in the FLAG-CaMKK2 immunoprecipitate was p-ACC, a downstream target of activated AMPK, and CaM, which is required for CaMKK2 activity. The association between CaMKK2, AMPK, ACC, and CaM disappeared when the metal chelators EDTA and EGTA were included during cell lysis and immunoprecipitation, although the chelators had no effect on the ability to precipitate CaMKK2 (Figure 5C), suggesting that Ca^{2+}/CaM and/or MgATP are required for complex formation.

AMPK is believed to exist in cells predominantly as a heterotrimer composed of the α catalytic and the β and γ regulatory subunits, which function to stabilize, localize, and confer AMP

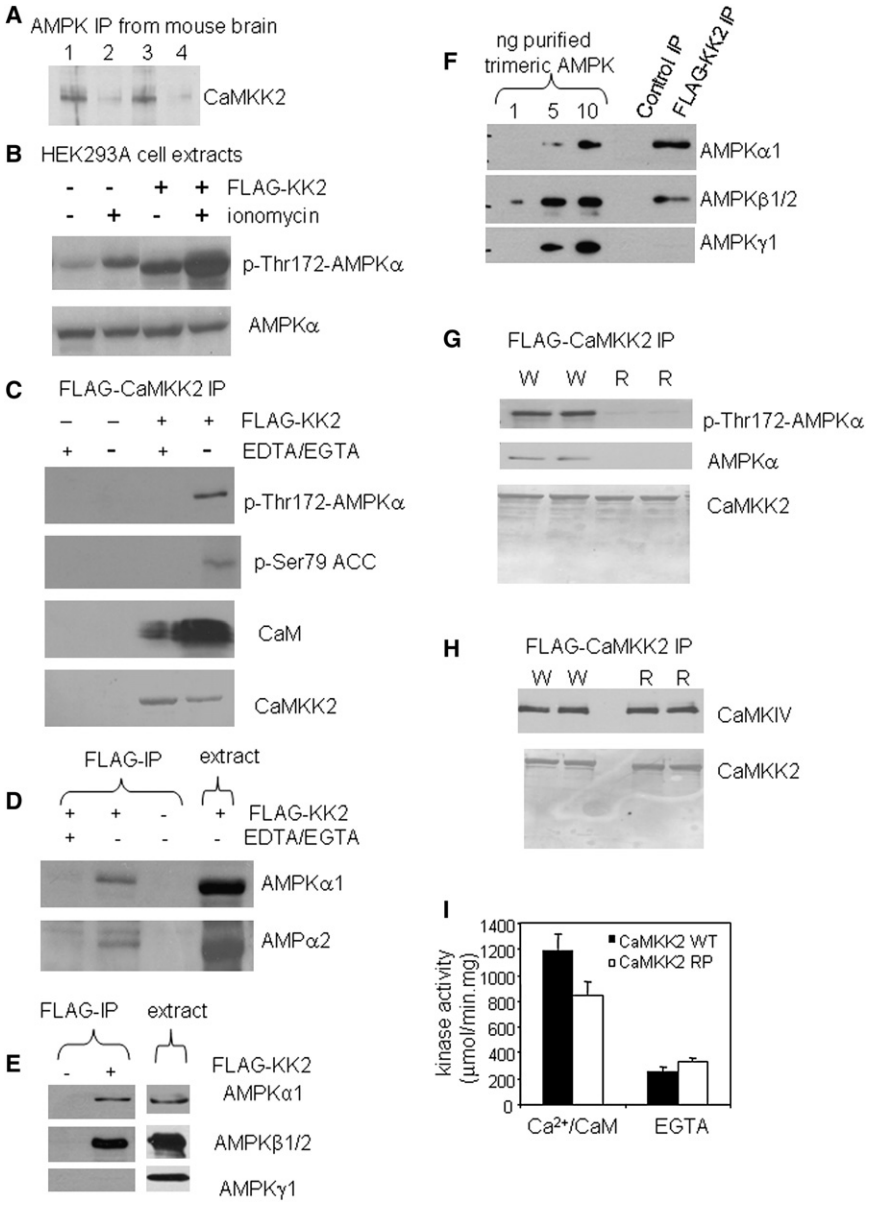

Figure 5. CaMKK2 Forms a Signaling Complex with AMPK

(A) CaMKK2 coimmunoprecipitates with AMPK from mouse brain. Brain extracts were incubated with AMPKα antibody (lanes 1 and 3) or preimmune serum (lanes 2 and 4). The immunoprecipitates were then immunoblotted for CaMKK2.

(B) FLAG-CaMKK2 increases basal and ionomycin-induced phosphorylation of AMPK. HEK293A cells transfected with FLAG-CaMKK2 or with control plasmid were treated with ionomycin or DMSO for 5 min. Cell extracts were then immunoblotted for p-Thr172 AMPKα and total AMPKα.

(C) CaMKK2 forms a physical complex with AMPK, ACC, and CaM. FLAG-CaMKK2 was immunoprecipitated from HEK293A cells transfected with either FLAG-CaMKK2 or with control plasmid, and the precipitates were immunoblotted for p-Thr172 AMPKα, p-Ser79 ACC, CaM, or CaMKK2. The presence of EDTA/EGTA during cell lysis and immunoprecipitation blocked formation of the complex.

(D) AMPKα1 and α2 physically associate with FLAG-CaMKK2. FLAG-CaMKK2 was immunoprecipitated with or without EGTA/EDTA from HEK293A cells that had been transfected with either FLAG-CaMKK2 or control plasmid. The precipitates were immunoblotted for the AMPKα1 and α2 subunits.

(E and F) The γ subunit of AMPK is not detected in the FLAG-CaMKK2/AMPK complex.

(E) HEK293A cell extracts or immunoprecipitated FLAG-CaMKK2 was immunoblotted for AMPKα1, β1/2, and γ1 subunits.

(F) FLAG-CaMKK2 immunoprecipitated from HEK293A cells and varying quantities of AMPK heterotrimer overexpressed and purified from bacteria were immunoblotted for AMPKα1, β1/2, and γ1 subunits.

(G) Deletion of the RP domain of CaMKK2 abolishes interaction with AMPK. FLAG-CaMKK2 WT (W) and RP deletion mutant (R) were immunoprecipitated from transfected HEK293A cells in the absence of EGTA/EDTA and immunoblotted for p-Thr172 AMPKα and total AMPKα. The bottom panel shows Coomassie staining of the CaMKK2 proteins.

(H) FLAG-CaMKK2 WT and RP deletion mutant were immunoprecipitated from transfected HEK293A cells as described in (F) and immunoblotted for CaMKIV (upper panel) or Coomassie stained (lower panel).

(I) The CaMKK2 RP deletion mutant is able to activate a fragment of AMPKα in vitro. Recombinant AMPKα 1–312 served as substrate for purified CaMKK2 WT and RP deletion mutant protein. Readout was ^{32}P-labeled phosphate transferred to SAMS peptide by activated AMPK. Data are presented as means ± SEM. n =3.

sensitivity to the catalytic subunit, and it is this heterotrimer which has been found to physically associate with LKB1. To determine the subunit composition of the AMPK present in the CaMKK2 complex, FLAG-CaMKK2 was immunoprecipitated from HEK293A cells and probed for the different subunits. Both isoforms of the AMPK catalytic subunit (α1 and α2) were identified in the absence, but not the presence, of metal chelators (Figure 5D), as were the β1/2 subunits (Figure 5E). However, the γ subunits were not detected, an observation confirmed using several γ subunit antibodies (Figure 5E and data not shown). In a related experiment, FLAG-CaMKK2 immunoprecipitated from HEK293A cells was compared with purified trimeric AMPK (Figure 5F) determined by Coomassie staining to be composed of stoichiometric amounts of α, β, and γ (data not shown). Although AMPKα and β were present in the CaMKK2 complex at levels similar to those observed in purified trimeric AMPK, once again γ was not detected. These results reveal that CaMKK2 may form a stable complex containing α catalytic and β structural subunits of AMPK but not the γ regulatory subunits.

The CaMKK RP domain, a 23-residue arginine/proline-rich insert between subdomains II and III of the kinase homology domain, has been previously shown to function as a protein-protein interaction domain in CaMKK1 (Tokumitsu et al., 1999). Deletion of this region from CaMKK2 produced a mutant protein that was unable to interact with AMPK in the coimmunoprecipitation

assay (Figure 5G), although the ability of the mutant to coimmunoprecipitate CaMKIV, another CaMKK2 substrate, remained unaltered (Figure 5H). When tested in vitro, the purified CaMKK2 RP deletion mutant could activate a fragment of the AMPK catalytic subunit (AMPK 1–312) similarly to WT CaMKK2 in the presence of saturating levels of Ca^{2+}/CaM and MgATP and a substrate excess of AMPKα 1–312 (Figure 5I). This not only demonstrates that removal of the RP domain does not abrogate the protein kinase activity of CaMKK2 but also suggests that stable complex formation between CaMKK2 and AMPK is not necessarily required for kinase-substrate interaction and may thus provide some other role in vivo.

DISCUSSION

Recent obesity and type 2 diabetes research suggests that some defects responsible for these conditions are due to altered responsiveness of key hypothalamic neurons to multiple metabolic cues such as leptin, ghrelin, insulin, glucose, and fatty acids. As a consequence, outputs emanating from these sites that are critical in regulating energy homeostasis become dysregulated. We provide evidence here that hypothalamic CaMKK2 mediates ghrelin-induced feeding. In the absence of CaMKK2, mice ate less and accumulated less body weight and fat stores when maintained on either low-fat or high-fat chow. The *CaMKK2* null animals expressed reduced levels of hypothalamic *NPY* and *AgRP* mRNAs and were unresponsive to the orexigenic effects of exogenously administered ghrelin. Furthermore, i.c.v. infusion of the selective CaMKK inhibitor STO-609 in adult WT mice resulted in the acute suppression of NPY expression and food intake. The resistance of *CaMKK2* null mice to suppression of food intake by STO-609 infusion provides compelling evidence that CaMKK2 is the direct target of the drug and that the specific inhibition of CaMKK2 in NPY neurons is likely responsible for the decreased level of *NPY* and *AgRP* mRNAs and feeding behavior.

Genetic and pharmacological data have demonstrated that NPY and AgRP, as well as the NPY neurons in the ARC of the hypothalamus where these neuropeptides are expressed, are key intermediaries in the ghrelin-induced feeding response (Cummings et al., 2005; Holst et al., 2005; Kojima et al., 1999; Kushi et al., 1998; Sun et al., 2004). Binding of ghrelin to Gq-coupled GHS-Rs expressed on NPY neurons leads to an increase in intracellular Ca^{2+} and the phosphorylation/activation of AMPK, each considered necessary for subsequent *NPY* gene induction (Andersson et al., 2004; Holst et al., 2005; Kohno et al., 2003; Kola et al., 2005). We hypothesize that CaMKK2 stimulates *NPY* expression by functioning as the AMPKK linking ghrelin-dependent Ca^{2+} signaling to AMPK activation. That the *CaMKK2* null mice described in this study exhibited reduced hypothalamic AMPK activity supports such a model.

We also present biochemical evidence for a CaMKK2-AMPK signaling complex. The two kinases associate in a complex also containing CaM, required for CaMKK2 activity, and ACC, a downstream target of AMPK. The AMPK and ACC present in the complex are phosphorylated on the appropriate residues, Thr172 and Ser79 respectively, demonstrated by others to be necessary for *NPY* gene induction in the hypothalamus and appetite stimulation (Hu et al., 2005). Our data suggest a model in which CaMKK2 interacts with the AMPKα subunit by substituting for the AMPKγ subunit through a mechanism requiring the RP domain of CaMKK2. The AMPKα subunit is unstable unless bound to the regulatory $\beta\gamma$ heterodimer, as deletion of either β or γ markedly decreases the in vivo level of AMPKα (Crute et al., 1998; Dyck et al., 1996). Our data suggest that CaMKK2 association with the AMPKα/β heterodimer provides an alternate means of stabilizing AMPK, confers Ca^{2+} sensitivity and AMP independence to the kinase, and is therefore fundamentally different from the AMP-dependent LKB1-AMPK complex.

The hypothesis that CaMKK2 controls appetite by regulating NPY signaling in the hypothalamus predicts that *CaMKK2* and *NPY* null mice will share the same metabolic phenotype. That reduced refeeding after a fast is a behavior characteristic of NPY depletion in mice that is phenocopied in *CaMKK2* null animals (Figure 3A) supports this hypothesis. On the other hand, *NPY/NPY-Y* null mice display a surprising lack of additional, predicted metabolic phenotypes. For example, when fed ad libitum, these animals have normal appetite, normal or increased body weight, increased adiposity, and increased serum leptin (Erickson et al., 1996; Kushi et al., 1998; Mashiko et al., 2003; Pedrazzini et al., 1998; Segal-Lieberman et al., 2003). This discrepancy has been suggested to result from compensatory mechanisms that rewire brain circuits during development (Kalra and Kalra, 2004). Similarly, we found that despite diminished *NPY* levels, *CaMKK2* null mice also showed normal appetite, slightly increased body weight, increased adiposity, and increased levels of circulating leptin and in these ways closely matched *NPY/NPY-Y* null mice (see Figure S1 available online), but only while fed Purina 5001 chow on which their parents were bred and raised. Once *CaMKK2* null mice were switched to the Surwit diet, they began to eat less and accumulated less body weight and fat on either low-fat or high-fat chow. Our data suggest that, like *NPY* null animals, *CaMKK2* null mice develop pathways to compensate for diminished NPY signaling, and these pathways function to prevent eating disorders as long as the animals are fed Purina 5001 chow. Once on the low- or high-fat Surwit diets, the compensatory pathways acquired by *CaMKK2* null mice are apparently no longer effective, and the feeding defects predicted from low NPY are exposed.

An intriguing phenotypic consequence of depleting CaMKK2 was observed in animals maintained on the high-fat diet, as these mice were protected from the hyperglycemia and insulin resistance that developed in WT controls over the course of several months. Although the mechanism responsible for the improved glucose handling is unknown, there are several possibilities. Since obesity represents the leading risk factor for the development of hyperglycemia (and type 2 diabetes), the improvements observed in *CaMKK2* null mice may result directly from them accumulating less body weight and fat stores compared to WT mice prior to glucose and insulin testing (Golay and Ybarra, 2005). Improved glucose tolerance is also consistent with enhanced leptin signaling (Elmquist et al., 2005), implicated in *CaMKK2* null mice by decreased hypothalamic AMPK activity (Minokoshi et al., 2004). In fact, it is possible that enhanced leptin signaling in *CaMKK2* null mice may contribute as well to the observed decreases in food intake and body weight gain.

One major factor contributing to the onset of obesity in mammals is the leptin resistance that develops as leptin levels rise in

response to an increase in fuel stores. This is believed to occur at the level of the blood-brain barrier leptin transporter and/or Socs3-negative feedback regulation of leptin receptor signaling (Banks, 2003; Munzberg and Myers, 2005). If, as we hypothesize, CaMKK2 directly regulates hypothalamic AMPK activity, then *CaMKK2* null mice may enjoy enhanced leptin signaling unaffected by the typical changes that bring about leptin resistance. The recently reported haploinsufficient Socs3 mouse is another example where the suppression of leptin sensitivity by high-fat diet can be overcome by genetically altering hypothalamic leptin signaling, in this case through a decrease in the Socs3-mediated negative feedback regulation of the leptin receptor (Mori et al., 2004). High-fat diet-induced leptin resistance can also be bypassed in mice by the pharmacological administration of CNTF, which activates leptin signaling through a mechanism involving a decrease in hypothalamic AMPK activity (Steinberg et al., 2006). Indeed, perhaps the central CaMKK2/AMPK signaling axis is necessary for the development of insulin resistance, which would contrast markedly with activation of AMPK in peripheral tissues, as this is associated with increased insulin sensitivity.

We also cannot rule out the possibility that CaMKK2 regulates glucose homeostasis through direct action in the periphery. Islet cells in the pancreas are known to express GHS-R and to respond to ghrelin by blocking insulin secretion, which promotes hyperglycemia (Cummings et al., 2005). To our knowledge, the expression of CaMKK2 in islet cells has not been evaluated, but, if present, the kinase might mediate the response to ghrelin as we hypothesize occurs in the hypothalamus. GHS-R antagonists have been shown to promote glucose tolerance in mice through action on islet cells while at the same time suppressing appetite and promoting weight loss through action in the hypothalamus (Esler et al., 2007). Collectively, in mice these antagonists produce all of the phenotypes observed by depleting CaMKK2.

In any event, the behavior of *CaMKK2* null mice on the high-fat diet underscores the value of targeting CaMKK2 as a possible therapeutic locus in the treatment of obesity and diabetes. Inhibition of CaMKK2 should selectively prevent AMPK activation in the ARC, where doing so should produce the desirable effects of reducing *NPY* gene induction and appetite. However, in peripheral metabolic tissues such as liver, muscle, and fat where abundant evidence indicates that activation, not inhibition, of AMPK is desirable for controlling obesity and diabetes (Hardie et al., 2003), CaMKK inhibitors are unlikely to have direct effects for at least two reasons. First, CaMKK protein expression in these tissues is absent or very low (Anderson et al., 1998). Second, LKB1 has been shown to function as the important AMPKK in these contexts (Sakamoto et al., 2005; Shaw et al., 2005). Finally, that depletion of CaMKK2 improves glucose tolerance while suppressing appetite and promoting weight loss is a somewhat unusual and quite desirable combination, as most current treatments for type 2 diabetes promote weight gain—in turn a major risk factor for the disease.

EXPERIMENTAL PROCEDURES

Animal Care

All animals were bred and maintained in either the Duke University Levine Science Research Center or Vivarium animal facilities under a 12 hr light (0600–1800)/12 hr dark (1800–0600) cycle. Food and water were provided ad libitum, and all animal care was in compliance within National Institutes of Health and institutional guidelines on the care and use of laboratory and experimental animals.

Targeted Deletion of the Mouse *CaMKK2* Locus

The *CaMKK2* gene was targeted by homologous recombination in embryonic stem (ES) cells using the triple-lox/*CaMKK2* targeting construct generated from fragments of the *CaMKK2* gene from the mouse 129/SvJ strain genomic BAC library (Duke Genome Facility) and the triple-lox vector series created by R.T. Premont (Gainetdinov et al., 1999). The targeting construct introduced two loxP sites into the gene flanking exons 2–4, which encode elements of the CaMKK2 ATP binding domain, as well as the neo cassette, also flanked by loxP sites. A 7 kb HindIII fragment containing exon 1 (long recombination arm) and the 4 kb HindIII-SbfI fragment containing exons 2–4 (the gene fragment to be flanked by loxP sites) were ligated into the loxL vector. A 0.5 kb AscI-HindIII fragment (short recombination arm) was ligated into the loxC/diphtheria toxin vector. The appropriate restriction enzyme digests and ligation steps were performed to generate the final targeting construct containing the long recombination arm, floxed exons 2–4, the neo cassette, the short recombination arm, and the diphtheria toxin cassette (Gainetdinov et al., 1999). After identification of targeted ES cell clones by Southern analysis, the cells were transiently transfected with Cre recombinase to delete *CaMKK2* exons 2–4 and the neo cassette (confirmed by PCR analysis). Germline chimeras, generated by blastocyst injections, were crossed with C57BL/6 mice, and homozygous mutants and WT littermates were obtained from breeding of heterozygotes. Offspring were genotyped by PCR using forward primer 799–822, 5′-TCAGTCAGTCTCACAGTGCCAAGC-3′, and reverse primer 1992–1974, 5′-TTGAACTCCTGACCTTCGG-3′, which produces an ~900 bp band when exons 2–4 have been deleted and no specific band from the WT locus. Forward primer 257–278, 5′-CGTCTTTCTTTTTTTGGGGGTG-3′, and reverse primer 494–471, 5′-CCTTGTTTGGGGAATGTGGAATAG-3′, produce a 237 bp band from exon 2, thus detecting the WT locus. The WT and *CaMKK2* null mice used in the experiments reported herein were backcrossed three generations onto the C57BL/6J genetic background. The results presented in Figure 4 for WT male mice are very similar to those previously reported for isogenic C57BL/6J male mice (Surwit et al., 1988).

In Situ Hybridization

Brains were removed from 3-month-old mice, frozen in powdered dry ice, and stored at −80°C. Ten micrometer coronal sections, cut serially on a cryostat, were collected at the midregion of the hypothalamus (bregma −1.7), thaw mounted, and stored at −80°C until use. The slides were then processed for in situ hybridization by transferring directly into ice-cold 4% paraformaldehyde and fixing for 10 min at room temperature. After a 10 min wash in 2× SSC, sections were crosslinked for 5 min with an ultraviolet light placed 30 cm from the tissue. Prehybridization, hybridization, and washing steps were then performed as described previously (Anderson et al., 1998). RNA probes were synthesized as follows: cDNAs encoding PCR-generated fragments of *NPY*, *MCH*, and *CaMKK2* coding regions were subcloned into the polylinker of the pCR2 (Invitrogen) vector. The PCR primer pairs were forward primer 131–151 and reverse primer 665–646 for *CaMKK2*, 5′-CTCCGCTCTGCGAC ACCTAC-3′ (forward) and 5′-AATCAGTGTCTCAGGGCT-3′ (reverse) for *NPY*, and 5′-ATTCAAAGAACACAGGCTCCAAAC-3′ (forward) and 5′-CGGA TCCTTTCAGAGCGAG-3′ (reverse) for *MCH*. Runoff [S^{35}]UTP-labeled sense and antisense transcripts corresponding to base pairs −10–524 of *CaMKK2*, base pairs 220–294 of *NPY*, and base pairs 307–399 of *MCH* were generated using SP6 or T7 RNA polymerase according to the manufacturer's protocol (Promega). Unincorporated nucleotides were removed by washing the EtOH-precipitated RNA pellets with 70% EtOH.

Hypothalamic mRNA Quantification

Total RNA from hypothalamus was extracted using an RNeasy Mini Kit (QIAGEN) and quantified spectrophotometrically. Single-stranded cDNA was synthesized using SuperScript III RNase H Reverse Transcriptase (Invitrogen) according to the manufacturer's directions. Real-time PCR was carried out using an iCycler (Bio-Rad) with iQ SYBR Green Supermix (Bio-Rad) and the following primers: *AgRP*, 5′-GCGGAGGTGCTAGATCCA-3′ (forward) and

5′-AGGACTCGTGCAGCCTTA-3′ (reverse); *NPY*, 5′-CTCCGCTCTGCGAC ACTAC-3′ (forward) and 5′-AATCAGTGTCTCAGGGCT-3′ (reverse); *POMC*, 5′-ACCTCACCACGGAGAGCA-3′ (forward) and 5′-GCGAGAGGTCGAGTTTG C-3′ (reverse); *18S ribosomal protein*, 5′-AGGGTTCGATTCCGGAGAGG-3′ (forward) and 5′-CAACTTTAATATACGCTATTGG-3′ (reverse). After deriving the relative amount of each transcript from a standard curve, *NPY*, *AgRP*, and *POMC* transcript levels were normalized to *18S ribosomal RNA*.

AMPK Immunoprecipitation and Activity

Mouse hypothalamus was homogenized in Triton lysis buffer containing 20 mM Tris-Cl (pH 7.4), 50 mM NaCl, 50 mM NaF, 5 mM NaPPi, 250 mM sucrose, 1% Triton X-100, 1 mM DTT, 1 μg/ml leupeptin, 10 μg/ml pefabloc, 1 μg/ml aprotinin, and 100 nM okadaic acid. After pelleting the insoluble material, AMPKα was immunoprecipitated from protein-matched extracts using an antibody directed against residues 2–20 of the α subunit (Chen et al., 2003) and assayed on beads for AMPK activity against the SAMS peptide as described previously (Hurley et al., 2006).

Dual Energy X-Ray Absorptiometry

Mice were anesthetized (ketamine 100 mg/kg; xylazine 10 mg/kg) and scanned four times (with no repositioning between scans) using a Lunar PIXImus II densitometer (software version 2.0; GE Lunar Corp.). All mice were granted ad libitum access to food and water before dual energy X-ray absorptiometry (DEXA) measurements, which were typically performed between 0800 and 1130. Calibration of the instrument was conducted as recommended by the manufacturer. Briefly, an aluminum/Lucite phantom (total bone mineral density = 0.0594 g/cm^2, percentage fat = 12.4%) was placed on the specimen tray and measured four times without repositioning. The phantom was measured daily before animal testing to ensure quality control. Anesthetized mice were then placed on the imaging positioning tray in a prostrate fashion with the front and back legs extended away from the body. Heads were excluded from all analyses by placing an exclusion region of interest (ROI) over the head. Thus, all body composition data exclude the head.

Serum Hormone Analysis

Mice with unrestricted access to food and water were collected at 0900 and sacrificed by decapitation, and blood was collected from the trunk. Blood samples were centrifuged at 14,000 rpm at 4°C, and serum was flash frozen in liquid N_2. Radioimmunoassays (Linco Research) were used to quantify leptin, adiponectin, ghrelin, glycerol, and free fatty acids.

Glucose and Insulin Tolerance Assays

Glucose tolerance assays were performed on mice that were fasted overnight (>12 hr). At 0900, mice were measured for baseline glucose by collecting a small drop of blood from the tail vein for analysis using a handheld Bayer Ascensia Contour glucometer. After the baseline glucose values were established, each mouse was given an i.p. injection of 2 mg glucose/g body weight. Blood glucose was quantified as a function of time until glucose levels returned to near baseline values. Insulin tolerance was conducted using the same glucometer, also at 0900. Mice were fasted for 3 hr prior to starting the procedure. After the baseline glucose values were established, mice were given recombinant human insulin (1 U/kg i.p. Eli Lilly). Clearance of plasma glucose was subsequently monitored at 15, 30, and 60 min postinjection.

Cannulation and Infusion of STO-609

Insertion of cannulae (Plastics One) and subsequent infusion of solutions into the third ventricle of adult WT or *CaMKK2* null mice using Alzet osmotic minipumps (DURECT Corporation) were performed as follows. A stock solution of STO-609 (20 mM in 100 mM NaOH) was diluted 1:1000 in 0.9% sterile saline to obtain a 20 μM working concentration in 100 μM NaOH (pH ~ 7.0). One hundred microliters of STO-609 or carrier was loaded into individual osmotic minipumps (Alzet model 1007D) 12 hr prior to surgical implantation and allowed to equilibrate in 0.9% sterile saline at 37°C to ensure that the pumps began to work immediately after implantation at the maximal flow rate of 0.5 μl/hr. Prior to surgery, mice were administered ketamine 80 mg/kg; xylazine 10 mg/kg i.p. After the anesthetic had taken effect, mice were secured in a stereotaxic apparatus (Kopf Instruments), and an incision was made down the midline of the head to expose the skull. After swabbing the exposed skull with 95% EtOH to remove any contaminants, the bregma line was located and marked. A small access hole was drilled at bregma −1.94, and the cannula was inserted to a depth of 5.8 mm and secured with epoxy bone cement. After the bone cement dried, a small incision was made in the skin between the scapulae. A small pocket was formed in the subcutaneous tissue, and the pump was implanted and connected to the cannula via a small sterile plastic tube. The incision was then closed, and the animal was placed on a heating pad to recover. Mice were monitored daily for normal behavior over a 7 day period, at which time they were sacrificed, and the hypothalamus was removed for RNA extraction.

Immunoblotting

Samples were fractionated by SDS-PAGE and transferred to Immobilon-P membranes (Millipore). All blocking and secondary antibody incubation steps were performed in TBS containing 5% nonfat milk, while primary antibody incubations were performed in TBS containing 5% BSA. Washes were performed in TBS with 0.5% Tween 20. AMPKα anti-phospho-Thr172, anti-AMPKα, anti-AMPKα1, anti-AMPKα2, and ACC anti-phospho-Ser79 were used at 1:1000 dilution. Anti-AMPKβ1/2 (Epitomics, Inc., #1604-1) was used at 1:5000, and anti-AMPKγ1 (Epitomics, Inc., #1592-1) was used at 1:1000. Anti-CaMKK2 (Santa Cruz L-19, #sc-9629) was used at 1:200, anti-CaMKIV (BD Biosciences, #610276) was used at 1:2000, and anti-CaM (Upstate Biotechnology, #05-173) was used at 1:1000. Horseradish peroxidase-conjugated secondary antibodies were from Jackson ImmunoResearch Laboratories, Inc., and were used at 1:5000 with an ECL kit from Amersham Biosciences.

Cells, Cell Culture, Cell Transfection, and Cell Stimulation

The human embryonic kidney cell line QBI-293A (HEK293A) from Quantum Biotechnologies was cultured as recommended by the supplier. The immortalized mouse hypothalamic cell line N38 from CELLutions Biosystems was cultured as recommended by the supplier, except that charcoal-stripped FBS was used in the growth medium. Cells were transfected with pSG5-FLAG-CaMKK2 or empty pSG5 vector (Stratagene) using Lipofectamine 2000 reagent (Invitrogen) according to the manufacturer's recommendations and cultured 16–24 hr before stimulation with ionomycin. Extracts of HEK293A or N38 cells were prepared by scraping the cells in NP-40 lysis buffer containing 25 mM Tris-HCl (pH 7.4), 50 mM NaCl, 0.5% NP-40, 25 mM NaH_2PO_4, 2 mM EGTA, 2 mM EDTA, 50 mM NaF, 1 μg/ml aprotinin, 1 μg/ml leupeptin, 10 μg/ml pefabloc, and 100 nM okadaic acid. After 30 min on ice, insoluble material was pelleted by centrifugation at 14,000 × g for 20 min, and the supernatant was reserved for immunoblot analysis.

Immunocytochemistry to Detect NPY Protein in N38 Cells

N38 cells were cultured on glass coverslips. Following treatment with STO-609, ionomycin, or 2-DG, the cells were fixed for 10 min in 1% paraformaldehyde/PBS and washed and permeabilized for 10 min in 0.05% Triton X, 20 mM Tris (pH 7.4), 50 mM NaCl, 300 mM sucrose, and 3 mM $MgCl_2$. After permeabilization, the cells were washed and blocked for 20 min in 5% normal sheep serum/PBS and incubated overnight at 4°C with rabbit anti-NPY (Sigma, N9528) diluted 1:4000 in 5% sheep serum/PBS. The cells were washed and incubated in the dark for 1 hr with anti-rabbit Cy3 (Jackson ImmunoResearch Laboratories, Inc.) diluted 1:200 in 5% sheep serum/PBS, washed again, and mounted in hard-set mounting medium (Vectashield) with DAPI. All washing steps were performed in triplicate for 5 min with PBS, and the procedure was performed at room temperature except for the 4°C incubation with primary antibody.

CaMKK2-AMPK Coimmunoprecipitation and AMPK Heterotrimer Purification

Unstimulated transfected cells were harvested in NP-40 lysis buffer as described above with or without EDTA/EGTA as indicated, and the resulting supernatant was incubated for 2 hr at 4°C with 20 μl anti-FLAG M2 agarose (Sigma, A2220). The resin was washed 2× with NP-40 lysis buffer and 1× with TBS prior to elution of the FLAG-CaMKK2 protein in 40 μl TBS containing 300 ng/μl FLAG peptide (Sigma, F3290). The eluted protein was then analyzed by immunoblot. Recombinant trimeric AMPK was expressed and purified from bacteria as described previously (Neumann et al., 2003).

CaMKK2 Mutagenesis

The CaMKK2 RP deletion mutant was generated using the QuikChange Site-Directed Mutagenesis Kit (Stratagene) with rat *CaMKK2* WT cDNA as template and the primers 5′-CCAAAAAGAAGCTGATCCGAAGGGGCCCC ATCGAGCAGG-3′ (sense) and 5′-CCTGCTCGATGGGGCCCCTTCGGATCAG CTTCTTTTTGG-3′ (antisense). The nucleotide sequence of the entire cDNA was confirmed by automated sequencing (Duke University DNA Sequencing Facility).

In Vitro CaMKK2 Activity

FLAG-CaMKK2 WT and RP deletion mutant were expressed in HEK293A cells, immunoprecipitated, and eluted from FLAG resin as described above. After assessing protein purity and quantity by fractionating aliquots by SDS-PAGE along with γ-globulin standards and quantification of Coomassie-stained bands, activity was measured by adding FLAG-CaMKK2 to the reaction at a concentration of 4 nM, along with the substrate MBP-AMPKα 1–312 at 200 nM. When measuring Ca^{2+}/CaM-dependent activity, the reaction also contained 25 mM HEPES (pH 7.5), 0.1% Tween 20, 10 mM $MgCl_2$, 400 μM ATP, 1 μM CaM, 1 mM $CaCl_2$, 20 μM SAMS peptide, and 0.024 μCi/μl [γ-^{32}P]ATP. Ca^{2+}/CaM-independent activity was determined by including 2 mM EGTA in the reaction described above. Readout was the transfer of ^{32}P to SAMS peptide by activated AMPK, which was quantified by a phosphocellulose method as described previously (Anderson et al., 1998).

SUPPLEMENTAL DATA

Supplemental Data include one table and one figure and can be found with this article online at http://www.cellmetabolism.org/cgi/content/full/7/5/377/DC1/.

ACKNOWLEDGMENTS

The authors thank members of the Means, Kemp, and Witters laboratories for reagents, advice, and discussions. We are grateful to W. Wetsel and R. Rodriguez of the Duke Mouse Behavior Phenotyping Shared Resource for help with metabolic testing and ARC biopsies as well as C. Newgard and colleagues of the Duke University Sarah W. Stedman Nutrition and Metabolism Center for advice, serum assays, and critical reading of the manuscript. This work was supported in part by NIH grants to A.R.M. (GM033976) and L.A.W. (DK035712) as well as by the Australian Research Council, the National Heart Foundation of Australia, and the National Health and Medical Research Council of Australia to B.E.K. B.E.K. is an Australian Research Council Federation Fellow.

Received: May 16, 2007
Revised: January 7, 2008
Accepted: February 25, 2008
Published: May 6, 2008

REFERENCES

Anderson, K.A., Means, R.L., Huang, Q.H., Kemp, B.E., Goldstein, E.G., Selbert, M.A., Edelman, A.M., Fremeau, R.T., and Means, A.R. (1998). Components of a calmodulin-dependent protein kinase cascade. Molecular cloning, functional characterization and cellular localization of Ca2+/calmodulin-dependent protein kinase kinase beta. J. Biol. Chem. *273*, 31880–31889.

Andersson, U., Filipsson, K., Abbott, C.R., Woods, A., Smith, K., Bloom, S.R., Carling, D., and Small, C.J. (2004). AMP-activated protein kinase plays a role in the control of food intake. J. Biol. Chem. *279*, 12005–12008.

Bagnasco, M., Kalra, P.S., and Kalra, S.P. (2002). Ghrelin and leptin pulse discharge in fed and fasted rats. Endocrinology *143*, 726–729.

Banks, W.A. (2003). Is obesity a disease of the blood-brain barrier? Physiological, pathological, and evolutionary considerations. Curr. Pharm. Des. *9*, 801–809.

Broberger, C., and Hokfelt, T. (2001). Hypothalamic and vagal neuropeptide circuitries regulating food intake. Physiol. Behav. *74*, 669–682.

Chen, Z.P., Stephens, T.J., Murthy, S., Canny, B.J., Hargreaves, M., Witters, L.A., Kemp, B.E., and McConell, G.K. (2003). Effect of exercise intensity on skeletal muscle AMPK signaling in humans. Diabetes *52*, 2205–2212.

Clark, J.T., Kalra, P.S., Crowley, W.R., and Kalra, S.P. (1984). Neuropeptide Y and human pancreatic polypeptide stimulate feeding behavior in rats. Endocrinology *115*, 427–429.

Crute, B.E., Seefeld, K., Gamble, J., Kemp, B.E., and Witters, L.A. (1998). Functional domains of the alpha1 catalytic subunit of the AMP-activated protein kinase. J. Biol. Chem. *273*, 35347–35354.

Cummings, D.E., Weigle, D.S., Frayo, R.S., Breen, P.A., Ma, M.K., Dellinger, E.P., and Purnell, J.Q. (2002). Plasma ghrelin levels after diet-induced weight loss or gastric bypass surgery. N. Engl. J. Med. *346*, 1623–1630.

Cummings, D.E., Foster-Schubert, K.E., and Overduin, J. (2005). Ghrelin and energy balance: focus on current controversies. Curr. Drug Targets *6*, 153–169.

Dyck, J.R., Gao, G., Widmer, J., Stapleton, D., Fernandez, C.S., Kemp, B.E., and Witters, L.A. (1996). Regulation of 5′-AMP-activated protein kinase activity by the noncatalytic beta and gamma subunits. J. Biol. Chem. *271*, 17798–17803.

Elmquist, J.K., Coppari, R., Balthasar, N., Ichinose, M., and Lowell, B.B. (2005). Identifying hypothalamic pathways controlling food intake, body weight, and glucose homeostasis. J. Comp. Neurol. *493*, 63–71.

Erickson, J.C., Clegg, K.E., and Palmiter, R.D. (1996). Sensitivity to leptin and susceptibility to seizures of mice lacking neuropeptide Y. Nature *381*, 415–421.

Esler, W.P., Rudolph, J., Claus, T.H., Tang, W., Barucci, N., Brown, S.E., Bullock, W., Daly, M., Decarr, L., Li, Y., et al. (2007). Small-molecule ghrelin receptor antagonists improve glucose tolerance, suppress appetite, and promote weight loss. Endocrinology *148*, 5175–5185.

Flier, J.S. (2004). Obesity wars: molecular progress confronts an expanding epidemic. Cell *116*, 337–350.

Friedman, J.M., and Halaas, J.L. (1998). Leptin and the regulation of body weight in mammals. Nature *395*, 763–770.

Gainetdinov, R.R., Bohn, L.M., Walker, J.K., Laporte, S.A., Macrae, A.D., Caron, M.G., Lefkowitz, R.J., and Premont, R.T. (1999). Muscarinic supersensitivity and impaired receptor desensitization in G protein-coupled receptor kinase 5-deficient mice. Neuron *24*, 1029–1036.

Golay, A., and Ybarra, J. (2005). Link between obesity and type 2 diabetes. Best Pract. Res. Clin. Endocrinol. Metab. *19*, 649–663.

Gropp, E., Shanabrough, M., Borok, E., Xu, A.W., Janoschek, R., Buch, T., Plum, L., Balthasar, N., Hampel, B., Waisman, A., et al. (2005). Agouti-related peptide-expressing neurons are mandatory for feeding. Nat. Neurosci. *8*, 1289–1291.

Hardie, D.G., Scott, J.W., Pan, D.A., and Hudson, E.R. (2003). Management of cellular energy by the AMP-activated protein kinase system. FEBS Lett. *546*, 113–120.

Hawley, S.A., Pan, D.A., Mustard, K.J., Ross, L., Bain, J., Edelman, A.M., Frenguelli, B.G., and Hardie, D.G. (2005). Calmodulin-dependent protein kinase kinase-beta is an alternative upstream kinase for AMP-activated protein kinase. Cell Metab. *2*, 9–19.

Heymsfield, S.B., Greenberg, A.S., Fujioka, K., Dixon, R.M., Kushner, R., Hunt, T., Lubina, J.A., Patane, J., Self, B., Hunt, P., and McCamish, M. (1999). Recombinant leptin for weight loss in obese and lean adults: a randomized, controlled, dose-escalation trial. JAMA *282*, 1568–1575.

Holst, B., Brandt, E., Bach, A., Heding, A., and Schwartz, T.W. (2005). Nonpeptide and peptide growth hormone secretagogues act both as ghrelin receptor agonist and as positive or negative allosteric modulators of ghrelin signaling. Mol. Endocrinol. *19*, 2400–2411.

Hu, Z., Dai, Y., Prentki, M., Chohnan, S., and Lane, M.D. (2005). A role for hypothalamic malonyl-CoA in the control of food intake. J. Biol. Chem. *280*, 39681–39683.

Hurley, R.L., Anderson, K.A., Franzone, J.M., Kemp, B.E., Means, A.R., and Witters, L.A. (2005). The Ca2+/calmodulin-dependent protein kinase kinases are AMP-activated protein kinase kinases. J. Biol. Chem. *280*, 29060–29066.

Hurley, R.L., Barre, L.K., Wood, S.D., Anderson, K.A., Kemp, B.E., Means, A.R., and Witters, L.A. (2006). Regulation of AMP-activated protein kinase by multisite phosphorylation in response to agents that elevate cellular cAMP. J. Biol. Chem. *281*, 36662–36672.

Kalra, S.P., and Kalra, P.S. (2004). NPY and cohorts in regulating appetite, obesity and metabolic syndrome: beneficial effects of gene therapy. Neuropeptides *38*, 201–211.

Kohno, D., Gao, H.Z., Muroya, S., Kikuyama, S., and Yada, T. (2003). Ghrelin directly interacts with neuropeptide-Y-containing neurons in the rat arcuate nucleus: Ca2+ signaling via protein kinase A and N-type channel-dependent mechanisms and cross-talk with leptin and orexin. Diabetes *52*, 948–956.

Kojima, M., Hosoda, H., Date, Y., Nakazato, M., Matsuo, H., and Kangawa, K. (1999). Ghrelin is a growth-hormone-releasing acylated peptide from stomach. Nature *402*, 656–660.

Kola, B., Hubina, E., Tucci, S.A., Kirkham, T.C., Garcia, E.A., Mitchell, S.E., Williams, L.M., Hawley, S.A., Hardie, D.G., Grossman, A.B., and Korbonits, M. (2005). Cannabinoids and ghrelin have both central and peripheral metabolic and cardiac effects via AMP-activated protein kinase. J. Biol. Chem. *280*, 25196–25201.

Kushi, A., Sasai, H., Koizumi, H., Takeda, N., Yokoyama, M., and Nakamura, M. (1998). Obesity and mild hyperinsulinemia found in neuropeptide Y-Y1 receptor-deficient mice. Proc. Natl. Acad. Sci. USA *95*, 15659–15664.

Lambert, P.D., Anderson, K.D., Sleeman, M.W., Wong, V., Tan, J., Hijarunguru, A., Corcoran, T.L., Murray, J.D., Thabet, K.E., Yancopoulos, G.D., and Wiegand, S.J. (2001). Ciliary neurotrophic factor activates leptin-like pathways and reduces body fat, without cachexia or rebound weight gain, even in leptin-resistant obesity. Proc. Natl. Acad. Sci. USA *98*, 4652–4657.

Luquet, S., Perez, F.A., Hnasko, T.S., and Palmiter, R.D. (2005). NPY/AgRP neurons are essential for feeding in adult mice but can be ablated in neonates. Science *310*, 683–685.

Mashiko, S., Ishihara, A., Iwaasa, H., Sano, H., Oda, Z., Ito, J., Yumoto, M., Okawa, M., Suzuki, J., Fukuroda, T., et al. (2003). Characterization of neuropeptide Y (NPY) Y5 receptor-mediated obesity in mice: chronic intracerebroventricular infusion of D-Trp(34)NPY. Endocrinology *144*, 1793–1801.

Minokoshi, Y., Alquier, T., Furukawa, N., Kim, Y.B., Lee, A., Xue, B., Mu, J., Foufelle, F., Ferre, P., Birnbaum, M.J., et al. (2004). AMP-kinase regulates food intake by responding to hormonal and nutrient signals in the hypothalamus. Nature *428*, 569–574.

Mori, H., Hanada, R., Hanada, T., Aki, D., Mashima, R., Nishinakamura, H., Torisu, T., Chien, K.R., Yasukawa, H., and Yoshimura, A. (2004). Socs3 deficiency in the brain elevates leptin sensitivity and confers resistance to diet-induced obesity. Nat. Med. *10*, 739–743.

Morton, G.J., Cummings, D.E., Baskin, D.G., Barsh, G.S., and Schwartz, M.W. (2006). Central nervous system control of food intake and body weight. Nature *443*, 289–295.

Munzberg, H., and Myers, M.G., Jr. (2005). Molecular and anatomical determinants of central leptin resistance. Nat. Neurosci. *8*, 566–570.

Neumann, D., Woods, A., Carling, D., Wallimann, T., and Schlattner, U. (2003). Mammalian AMP-activated protein kinase: functional, heterotrimeric complexes by co-expression of subunits in Escherichia coli. Protein Expr. Purif. *30*, 230–237.

Pedrazzini, T., Seydoux, J., Kunstner, P., Aubert, J.F., Grouzmann, E., Beermann, F., and Brunner, H.R. (1998). Cardiovascular response, feeding behavior and locomotor activity in mice lacking the NPY Y1 receptor. Nat. Med. *4*, 722–726.

Petro, A.E., Cotter, J., Cooper, D.A., Peters, J.C., Surwit, S.J., and Surwit, R.S. (2004). Fat, carbohydrate, and calories in the development of diabetes and obesity in the C57BL/6J mouse. Metabolism *53*, 454–457.

Sakamoto, K., McCarthy, A., Smith, D., Green, K.A., Grahame Hardie, D., Ashworth, A., and Alessi, D.R. (2005). Deficiency of LKB1 in skeletal muscle prevents AMPK activation and glucose uptake during contraction. EMBO J. *24*, 1810–1820.

Segal-Lieberman, G., Trombly, D.J., Juthani, V., Wang, X., and Maratos-Flier, E. (2003). NPY ablation in C57BL/6 mice leads to mild obesity and to an impaired refeeding response to fasting. Am. J. Physiol. Endocrinol. Metab. *284*, E1131–E1139.

Shaw, R.J., Kosmatka, M., Bardeesy, N., Hurley, R.L., Witters, L.A., DePinho, R.A., and Cantley, L.C. (2004). The tumor suppressor LKB1 kinase directly activates AMP-activated kinase and regulates apoptosis in response to energy stress. Proc. Natl. Acad. Sci. USA *101*, 3329–3335.

Shaw, R.J., Lamia, K.A., Vasquez, D., Koo, S.H., Bardeesy, N., Depinho, R.A., Montminy, M., and Cantley, L.C. (2005). The kinase LKB1 mediates glucose homeostasis in liver and therapeutic effects of metformin. Science *310*, 1642–1646.

Steinberg, G.R., Watt, M.J., Fam, B.C., Proietto, J., Andrikopoulos, S., Allen, A.M., Febbraio, M.A., and Kemp, B.E. (2006). Ciliary neurotrophic factor suppresses hypothalamic AMP-kinase signaling in leptin-resistant obese mice. Endocrinology *147*, 3906–3914.

Sun, Y., Wang, P., Zheng, H., and Smith, R.G. (2004). Ghrelin stimulation of growth hormone release and appetite is mediated through the growth hormone secretagogue receptor. Proc. Natl. Acad. Sci. USA *101*, 4679–4684.

Surwit, R.S., Kuhn, C.M., Cochrane, C., McCubbin, J.A., and Feinglos, M.N. (1988). Diet-induced type II diabetes in C57BL/6J mice. Diabetes *37*, 1163–1167.

Tokumitsu, H., Takahashi, N., Eto, K., Yano, S., Soderling, T.R., and Muramatsu, M. (1999). Substrate recognition by Ca2+/Calmodulin-dependent protein kinase kinase. Role of the arg-pro-rich insert domain. J. Biol. Chem. *274*, 15803–15810.

Tokumitsu, H., Inuzuka, H., Ishikawa, Y., Ikeda, M., Saji, I., and Kobayashi, R. (2002). STO-609, a specific inhibitor of the Ca(2+)/calmodulin-dependent protein kinase kinase. J. Biol. Chem. *277*, 15813–15818.

Witters, L.A., Kemp, B.E., and Means, A.R. (2006). Chutes and Ladders: the search for protein kinases that act on AMPK. Trends Biochem. Sci. *31*, 13–16.

Woods, A., Dickerson, K., Heath, R., Hong, S.P., Momcilovic, M., Johnstone, S.R., Carlson, M., and Carling, D. (2005). Ca2+/calmodulin-dependent protein kinase kinase-beta acts upstream of AMP-activated protein kinase in mammalian cells. Cell Metab. *2*, 21–33.

Zamboni, M., Mazzali, G., Zoico, E., Harris, T.B., Meigs, J.B., Di Francesco, V., Fantin, F., Bissoli, L., and Bosello, O. (2005). Health consequences of obesity in the elderly: a review of four unresolved questions. Int. J. Obes. (Lond.) *29*, 1011–1029.